TECHNICAL ARTICLE

Calibration of a Digital Image Correlation System

C. Sebastian[1,2] and E.A. Patterson[1,2,3]

1 Composite Vehicle Research Center, Michigan State University, East Lansing, MI, USA
2 Department of Mechanical Engineering, Michigan State University, East Lansing, MI, USA
3 Department of Chemical Engineering and Materials Science, Michigan State University, East Lansing, MI, USA

Keywords
Digital Image Correlation, Optical Methods, Calibration, Reference material

Correspondence
C. Sebastian,
Department of Mechanical Engineering,
Michigan State University
East Lansing, MI, USA
Email: cmsebast@liv.ac.uk

Received: February 3, 2011; accepted: October 26, 2012

doi:10.1111/ext.12005

Abstract

The use and results of the procedure published by Standardisation Project for Optical Techniques of Strain measurement (SPOTS) for a successful calibration of a digital image correlation (DIC) system are described. The details of the calibration specimen used are discussed together with procedure and criteria that must be met to achieve an acceptable calibration. The DIC system was evaluated over a strain range of 289 to 2110 μstrain, with a resulting calibration uncertainty ranging from 14 to 28.7 μstrain. The optical strain measurements were obtained from images taken directly from the bare metal surface, which had been prepared with grit paper, as opposed to generating a speckle pattern by painting the surface.

Introduction

Although full-field optical strain analysis techniques such as digital image correlation (DIC) are widely used in the experimental mechanics field, the stress analysis community and industry in particular seem to be somewhat reluctant to adopt these methods for use alongside computational techniques. However, the drive to create lighter-weight, more efficient structures has led to many structures being optimized based on largely un-validated computational models which is of high-risk and undesirable. ASME V&V 10-2006[1] specifies the requirements for validation in computational solid mechanics without providing an approach.

Often a limited validation is performed by checking a few ''hot spots'' with strain gages without reviewing the whole structure. Full-field optical methods like DIC have the potential to provide data-rich maps of strain to support the validation of these computational models and thus provide confidence to designers. Despite this enormous potential, the stress analysis community has been slow to adopt such an approach.

One possible explanation is the almost complete lack of standards or accepted methodologies for processes such as calibration of the optical instruments. The few that do exist tend to be industry and instrument specific and leave the decision of what is acceptable or not to the user.[2] Calibration of the strain measurement system is an essential step in acquiring data for the validation of computational models. The recently published guide from the Standardisation Project for Optical Techniques of Strain measurement (SPOTS) seeks to change this by providing a universally appropriate calibration procedure for static and pseudostatic experiments.[3,4]

The calibration of a commercially available DIC system (Dantec Dynamics Q-400, Ulm, Germany) presented here was performed following the guidelines set forth by the SPOTS group. This article describes the practical knowledge necessary to perform a calibration of a DIC system, and presents the results of such a calibration.

Calibration Using a Reference Material

Calibration is ''the set of operations which establish, under specified conditions, the relationship between values indicated by a measuring instrument or system . . . and the corresponding values of a quantity realized by a reference standard'' and ''permits the estimation of errors of indication of the measuring instrument.''[5] In general, the calibration process

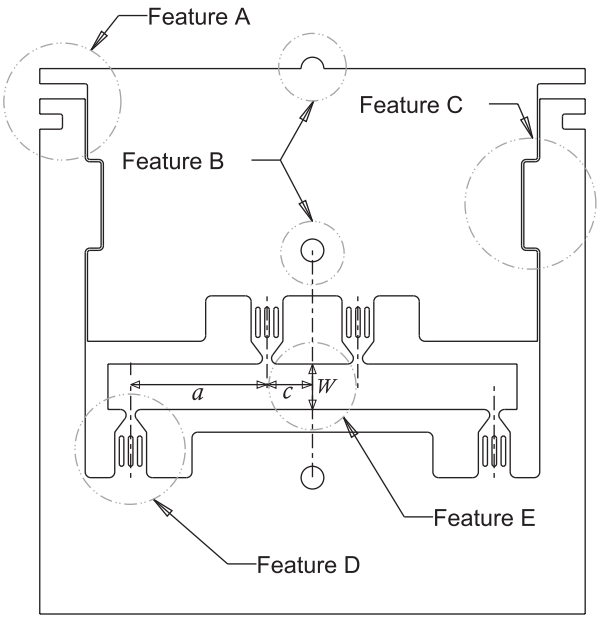

Figure 1 Drawing of the reference material showing some of the design features. A: Measurement tabs. B: Mounting holes for tensile loading and semi-circle for compressive loading. C: Interlock to prevent overload. D: Whiffle tree that allows for monolithic manufacturing of the specimen. E: Gage section.

involves a reference material, which is defined as ''a material or substance one or more properties of which are sufficiently well-established to be used for calibration of an apparatus''[5] and provides traceability via an unbroken chain of comparisons to an international or national standard. The SPOTS reference material is designed to produce a known strain field that can be related to the international standard for length, that is the meter. In order to establish the design, the SPOTS consortium used the rational decision-making process to identify 5 essential attributes (easy optical access, lack of hysteresis, an in-plane strain field, traceability to an international standard, and utilization of the length standard for traceability) and 24 desirable attributes of a reference material for the assessment of a full-field optical system for strain measurement.[3] These attributes were used to assess a large number of candidate designs for the reference material and resulted in the selection of the design shown in Fig. 1, which consists of a central beam loaded in symmetrical four-point bending.

The reference material has several noteworthy design features. Reproducibility between experiments and between laboratories was a major concern of the SPOTS group, which has been addressed by making the specimen and loading frame monolithic. The beam and the loading frame are therefore machined from a single piece of material. The specimen is designed such that the user has options for applying and measuring displacement loading. Feature A in Fig. 1 shows the tabs which allow the use of a variety of measurement devices that need to have been calibrated with respect to the standard for length in order to provide traceability. Feature B shows the holes for tensile loading of the specimen as well as the half-cylinder at the top to ensure proper alignment in the case of compressive loading. Feature C is a simple design feature that serves as an interlock to prevent an overload to the reference material which could cause plastic deformation. Feature D is one of the ''whiffle-trees'' which supports the beam. Ideally, rollers or knife edges would be used to minimize the transmission of lateral and rotational forces, but the monolithic design makes their use difficult. The constraint imposed by the use of the whiffle-trees causes a change in the strain in the gage section of the beam compared to the standard analytical solution for a beam subject to bending, so that strain in the transverse (x) direction is given by:

$$\varepsilon_{xx} = \frac{v_{\text{avg}}}{6W^2}(ky + \eta) \tag{1}$$

The correction factors are k and η which are unknown and must be found either through experimentation or analysis. An experimental procedure is used here and is explained in more detail in the next section. Finally, Feature E in Fig. 1 is the gage section, which is the area between the two inner loading points where the bending moment is constant along the length of the beam. The strain is measured in this region using the instrument being calibrated and the results compared to the analytical solution. A linear least square fit is used to analyze the differences between the two quantities, producing two parameters, α and β. The SPOTS guidelines provide a detailed procedure for this comparison and for determining the calibration uncertainty which has been followed here.

Experimental Setup and Procedure

Reference material

The reference material used for this calibration procedure was manufactured using electric discharge machining (EDM) from a single piece of 5-mm thick 2024-T351 aluminum. The specimen beam depth (W) was 15 mm. The gage section of the calibration specimen is shown in Fig. 1, and illustrates the dimensions W, a, and c. The values for these dimensions are listed in Table 1.

Table 1 The critical dimensions of the calibration specimen and their associated uncertainties

Parameter (units)	Nominal value	Uncertainty, u
W (mm)	15	0.017
a (mm)	45	0.017
c (mm)	15	0.017
ν_{avg} (μm)	27.5, 110, 218	0.89
k (—)	0.986	0.006
η (mm)	−0.068	0.006

Determination of the correction factors k and η

There were two steps in the calibration process: one to determine the correction factors described in Eq. (1), and the second to acquire the strain data with the instrument being calibrated. For both steps, the specimen was mounted in the servo-hydraulic test machine (MTS 810, Eden Prairie, MN, USA) using the loading holes. This arrangement allowed the specimen to be loaded in tension. The specimen was oriented upside down in the load frame relative to Fig. 1 and the usual orientation in guidelines. This minimizes the rigid body movement of the specimen relative to the camera. To measure the applied displacement in the specimen, two aluminum blocks were machined to hold a pair of digital displacement indicators (Mitutoyo 543-392, Kawasaki-shi, Japan) on each side of the specimen. The calibration results were evaluated using the unit of length; so it is important that displacement measurement devices have a calibration history traceable to an international standard. In this case, the indicators were purchased with calibration certificates which provide traceability to the National Institute of Standards and Technology (NIST). The certificates provide a level of expanded uncertainty for each of the indicators, which was taken into account when calculating the overall uncertainty of the system.

Figure 2 shows the calibration specimen installed in the test machine with the digital indicators attached using the custom mounting blocks. Strain gages (Vishay EA-13-120LZ-120/E, Raleigh, NC, USA) were bonded to the top and bottom surfaces of the gage section. The relatively small (5 mm) thickness of the specimen meant that single axis gages had to be used. Figure 3 shows the location of the strain gages on the specimen. The strain measurements were acquired using two digital strain indicators (Measurements Group P-3500, Raleigh, NC, USA). To find the correction factors k and η described earlier, it was necessary to acquire data from the strain gages as a function of applied displacement to the specimen. For this, the test machine was operated in displacement control, and readings were taken from the strain gages. In this way, approximately 30 strain measurement readings were obtained as a function of the applied displacement load.

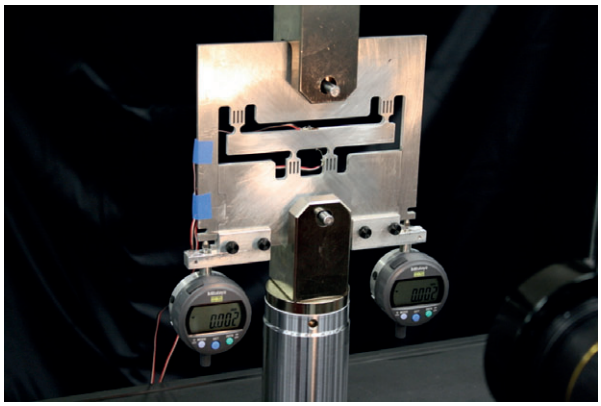

Figure 2 Close-up of the reference material installed ''upside-down'' in the MTS load frame. The digital indicators are mounted to the specimen by custom-machined mounting blocks.

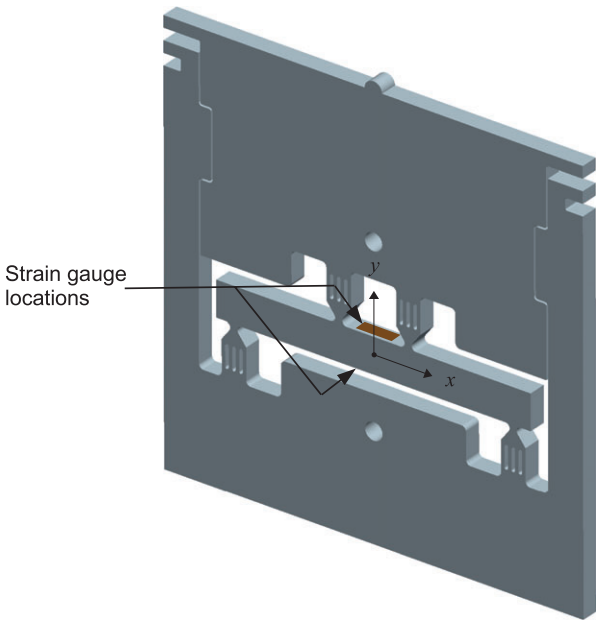

Figure 3 Rendered three-dimensional model of the reference material showing the strain gage locations and the reference coordinate system.

Calibration measurements

It was desired to calibrate a certain experimental setup for measuring strain fields, which consisted of a commercial DIC system outfitted with a particular lens and lighting apparatus. The reference material

of an appropriate size was selected for the setup being evaluated. During the experimental setup, the practical considerations for DIC measurements described by Sutton et al.[6] were used as a guide to obtain high-quality results, including optics and camera selection, lighting, surface pattern, and exposure time.

Recently, bare metal surfaces have been used successfully for DIC instead of applying a coating. For example, to study crack propagation in an aluminum alloy by Lopez-Crespo et al.[7,8] and for high temperature DIC measurements by Grant et al.[9] Previously, a similar technique had been used to measure displacements in bone samples subject to load.[10,11] The reference material was prepared in this fashion by first sanding the surface with 220 (P220) grit and then 400 (P700) grit paper. This yielded a high contrast pattern for the DIC images, a typical image of which is shown in Fig. 4.

A macro lens (Tamron SP 90 mm F/2.8 1:1 macro, Saitama-city, Japan) was fitted to the DIC camera which made it possible to fill the camera's field of view with the gage section of the specimen. To provide bright, uniform illumination of the specimen, a fiber optic ring light (Edmund Optics 58-839, Barrington, NJ, USA) and illuminator (Dolan-Jenner DC-950H, Boxborough, MA, USA) were used. The ring light was used in place of the standard LED floodlight because when the latter was used with the highly reflective bare metal surface it tended to produce glare. The camera and lens were positioned perpendicular to the surface of the gage section at a distance of 265 mm.

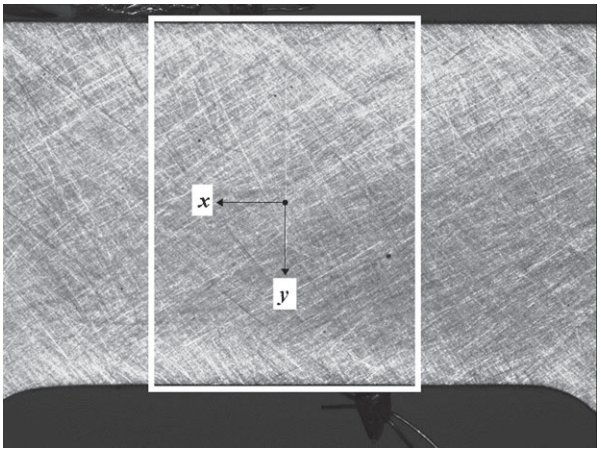

Figure 4 Photograph of the gage section showing the pattern produced on the surface of the specimen by using grit paper. The 11.2 mm by 15 mm rectangular area highlighted indicates the approximate gage section of the specimen.

The SPOTS procedure states that for a proper calibration test setup, the gage section of the beam should fill 90% of the short dimension of the detector, with at least a resolution of 10×10 pixels. The detector used for this calibration has a resolution of 1040×1392 pixels, which for 90% coverage of the short dimension yields an area of approximately 1.3 million pixels and a spatial resolution of approximately 84 pixels/mm. The procedure also states that the applied displacement be over a range between 10% and 90% of the maximum allowable load. The minimum slit diameter that can be typically manufactured using EDM for the interlock (C in Fig. 1) is the maximum allowable deflection for a beam with a depth of 15 mm (see Appendix A of the SPOTS Guidelines at http://www.opticalstrain.org). This value is typically between 0.25 and 0.30 mm, which gives a maximum allowable displacement range between 225 and 270 μm. To avoid damage to the specimen, a maximum displacement value of 225 μm was chosen.

To ensure a correct initial displacement reading, the digital indicators were installed in their proper locations and zeroed with the specimen laying flat on a laboratory bench. This prevented the weight of the indicators from imposing a displacement load on the system. The specimen was then mounted into the test machine and a 1–2 μm displacement preload applied to remove any slack in the system prior to applying the calibration load. The test machine control software (MTS Station Manager, MTS, Eden Prarie, MN, USA) was set to apply the load at a rate of 0.3 mm/min and the DIC system was programmed to record images at 2-s intervals. To capture the displacement measurements from the digital indicators as the specimen was being loaded, the DIC system's second camera (normally used for 3D measurements) was positioned to capture the values displayed by both indicators. This provided an exact displacement measurement corresponding to each image captured of the gage section of the specimen. Using this procedure resulted in approximately 30 data points over the entire displacement loading range. However, the SPOTS procedure only requires three data points at nominally equal increments spread between 10% and 90% of the maximum allowable load. The three displacements that were used for the analysis were 27.5, 110, and 218 μm. These values were chosen in part to allow comparison of the results to those from a previous calibration of an electronic speckle pattern interferometer.[12]

The images were processed using a commercially available DIC software code (Istra4D, Dantec

Dynamics). The software permits the image to be subdivided into subsets or facets, which the correlation algorithm tracks from one image to the next using the gray value pattern.[13] For this analysis the facet size was 31 pixels, with a 50% overlap between the facets. The correlation algorithm is based on a pseudoaffine coordinate transformation consisting of translation, stretch, shear, and distortion, along with photogrammetric corrections.[14] The determination of the intrinsic and extrinsic parameters was performed by a routine in the software using a target with a black and white checker pattern.

Results and Discussion

Correction factors and their uncertainty

The SPOTS procedure gives values for the correction factors from finite element analysis, but it also allows them to be found experimentally, as was done in this study. The values of the strain parallel to the neutral axis, $(\varepsilon_{xx})_{y=\pm\frac{W}{2}}$ obtained from the strain gages on the top and bottom surfaces of the beam were plotted in order to find the constraint correction factors k and η. Figure 5 shows the quantities $(\varepsilon_{xx})_{y=\frac{W}{2}} + (\varepsilon_{xx})_{y=-\frac{W}{2}}$ and $(\varepsilon_{xx})_{y=\frac{W}{2}} - (\varepsilon_{xx})_{y=-\frac{W}{2}}$ plotted as a function of applied displacement load between 0 and 180 μm. The correction factors k and η were determined from the coefficients resulting from a linear fit to the data. Using this method, k was found to be 0.986 and η was −0.068. The results from the finite element analysis given in the SPOTS guidelines are that for a beam depth ranging from 15 to 30 mm that $k = 0.94$ and η varies linearly from −0.10 to −0.18. The slightly higher k value indicates that the specimen had slightly less rotational constraint than the finite element model, and the smaller η value indicates less translational constraint in the x-direction. Table 1 lists the values found for the correction factors as well as their associated uncertainty, which was calculated from the variance of the fitted line.

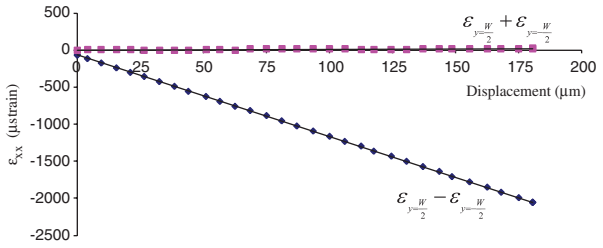

Figure 5 Plot of the strain from the gages mounted to the top and bottom surfaces of the specimen. A linear fit was applied to the data to determine the correction factors k and η.

Specimen dimensions and uncertainty

For this calibration, the uncertainty in these dimensions of the reference material was calculated from the manufacturing tolerances, which is specified as 0.05 mm by the SPOTS guidelines. However, an alternative way to determine the uncertainty would be to measure the geometry using a series of independent observations, and then calculate the mean and standard deviation from the measurements. The uncertainty for the applied displacement was a function of the digital indicators, which were purchased with NIST calibration certificates. The certificates provided the measurement range and uncertainty for each indicator.

Measurement system results and uncertainty

Figure 6 shows the strain along the centerline of the gage section parallel to the applied load obtained from Eq. (1) and from the DIC system for the three displacement load steps. Figure 7 shows the data generated by the DIC system for the 218 μm load step. The deviations, d, were then calculated for each of the load steps by subtracting the measured strain, ε_{xx} from the strain predicted using Eq. (1).

A linear least-squares fit was then applied to the deviations, resulting in the fit parameters α and β shown in the following equation:

$$d_k = \alpha_k + \beta_k y \tag{2}$$

where the subscript k indicates the load step. The variance of α and β was also calculated and used to find the uncertainty for each fit parameter. The range formed by plus or minus twice the uncertainty creates a 95% CI for each of the parameters. These data are summarized in Table 2.

Next, the total uncertainty in the measured strain, ε_{xx} for the calibration was calculated using the root-sum-of-squares method. This quantity includes the uncertainty in the dimensions, material properties, and correction factors for the calibration specimen, as well as for the applied displacement measurements. The flowchart in Fig. 8 shows how each of these components contributes to the minimum measurement uncertainty for the system. For each of the three displacement load steps, the mean residual deviations $(\alpha_k + \beta_k y) \pm 2u(d_k)$ are plotted along with the expanded uncertainty of the calibration specimen, $\pm 2u_{CS}$, in Fig. 9. The quantity $2u(d_k)$ provides a 95% CI around the regression line for the deviations found from Eq. (2), and the area between $\pm 2u_{CS}$ indicates the uncertainty from the calibration specimen.

According to the SPOTS guideline, an appropriately calibrated instrument is the one in which there is

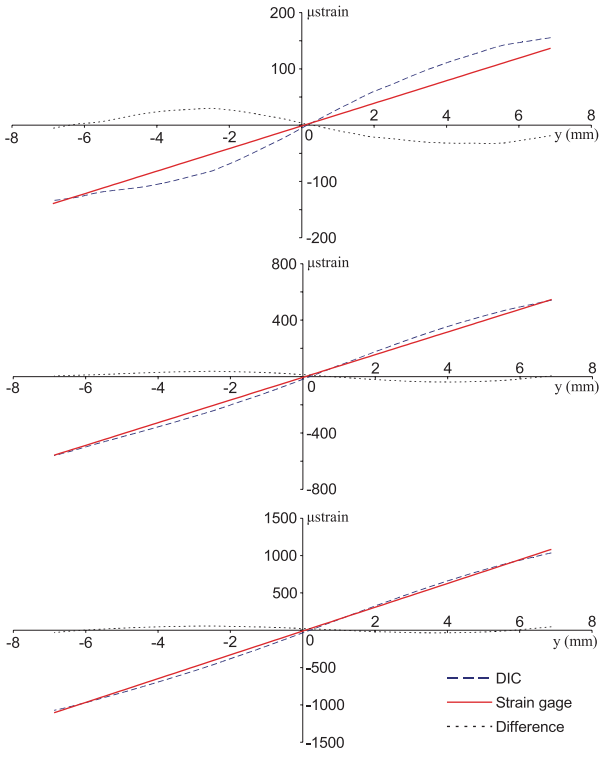

Figure 6 The measured and calculated ε_{xx} strain values along the center line of the gage section for each of the three displacement load steps: 27.5 μm (top), 110 μm (middle), and 218 μm (bottom).

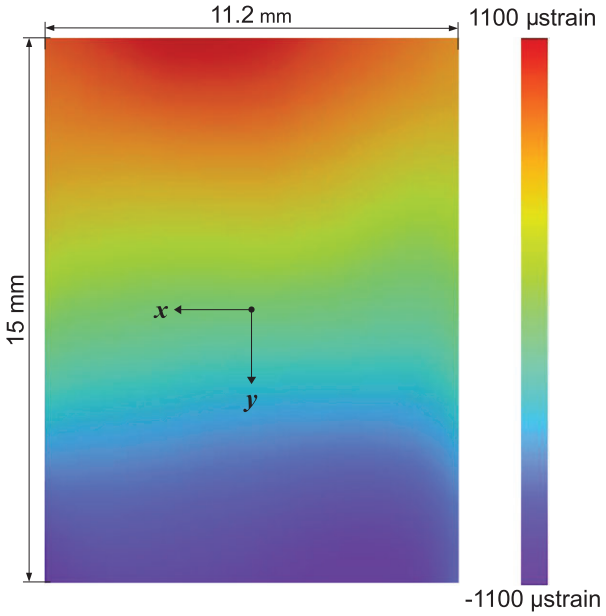

Figure 7 The *x*-component of the strain data generated by the DIC system for the 218 μm displacement load.

Table 2 Summary of the fit parameters calculated for each of the displacements, as well as their associated 95% CI

		Applied displacement ν_{avg} (μm)		
Fit parameter	Units	27.5	110	218
α	μstrain	−3.2	2.0	11.9
$u(\alpha)$	μstrain	1.3	1.7	2.7
95% CI (α)	μstrain	±2.57	±3.38	±5.36
β	μstrain/mm	−4.4	−4.9	−3.6
$u(\beta)$	μstrain/mm	0.3	0.4	0.7
95% CI (β)	μstrain/mm	±0.65	±0.85	±1.34

complete overlap between the expanded uncertainty of the reference material and the mean residual deviations $\alpha_k + \beta_k y$. In an ideal system, both α_k and β_k would be zero and no adjustments would be necessary. On the other hand, when $|\alpha_k|$ is less than twice its expanded uncertainty, $2u(\alpha_k)$, there is a statistically significant offset in the calibration. When $|\beta_k|$ is less than twice its expanded uncertainty, $2u(\beta_k)$, there is a statistically significant deviation in the calibration in which the deviations increase as a function of the distance, y from the center of the beam. It can be observed from Table 2 that there were no significant offsets or deviations with the exception of the 110 μm displacement where a significant offset was found.

The presence or otherwise of significant offsets or deviations is a useful diagnostic tool for improving the experimental setup of the calibrated instrument; however, diagnostics are not the primary purpose of a calibration which is to provide traceability to a standard and to evaluate the minimum measurement uncertainty. When the instrument is to be used to measure strain fields, as was the case in this instance, then it is appropriate to base the calibration on the results for strain; however, during a diagnostic process, it might be appropriate to consider components of the strain measurement process such as image acquisition and displacement calculations.

Overall system results and uncertainty

The resulting calibration uncertainty of the system, u_{CAL}, was found using the maximum strain value from each of the load steps and results from the combination of the uncertainties of the reference material and of the strain measurements. In order to better understand the significance of u_{CAL}, the relative uncertainty, u_{rel}, can be calculated which expresses u_{CAL} as a percentage of the measured strain value. Table 3 summarizes these values, which can be considered to be the minimum measurement

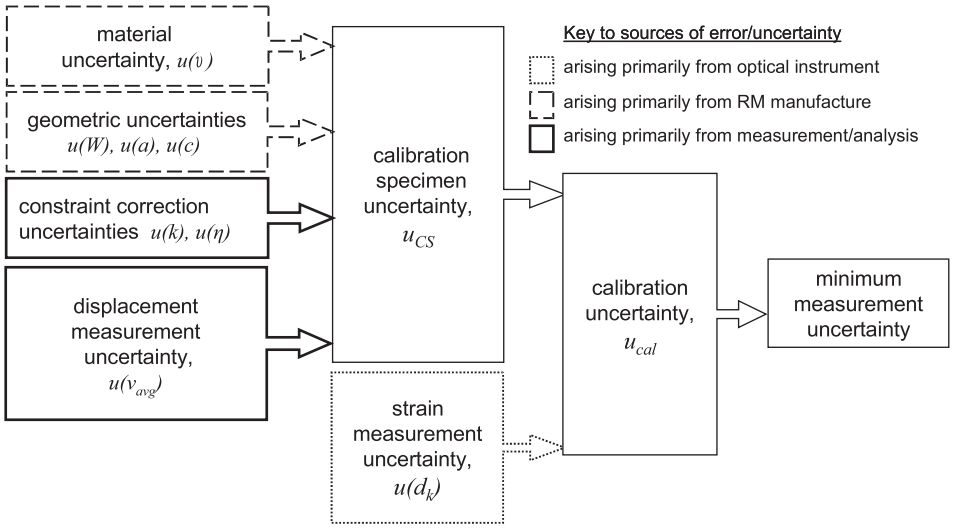

Figure 8 Flowchart showing the total measurement uncertainty of a system as a combination of uncertainties from the reference material and from the measurement system.

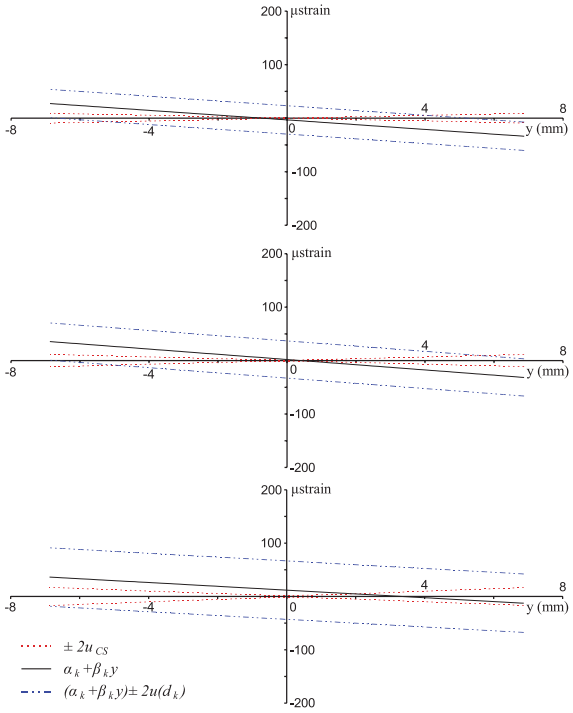

Figure 9 Plots of the expanded uncertainty of the reference material u_{CS} along with the mean residual deviations $\alpha_k + \beta_k y$ and the scatter band around the deviations $\pm 2u(d_k)$ for each load step: 27.5 μm (top), 110 μm (middle), and 218 μm (bottom).

uncertainty that would be expected in future strain measurements made with the calibrated instrument.

There were some challenges encountered during the calibration procedure that had to be overcome in order to achieve acceptable results. In comparison to Whelan et al.,[12] the specimen used for this calibration had a thickness of 5 mm as compared to 10 mm. The greater thickness allowed Whelan et al. to use strain gage rosettes, where it was only practical to use single axis gages for this specimen. The lack of a rosette meant that care had to be taken to ensure that the gages were aligned properly on the specimen. It was also found that the thin specimen did not stand upright on its own very well, making it difficult to load in compression. While testing the specimen in tension works just as well, it is slightly more difficult to mount it for tensile testing than for compression testing. In the interest of accuracy, the tolerances for the mounting holes and pins was fairly tight, so it usually took a few minutes of careful adjustment to get everything to align correctly to allow the insertion of the pins.

Another challenge was to obtain accurate strain measurements at the smallest load displacement step, 27.5 μm. An example of an initial measurement that was taken at this displacement is shown in Fig. 10. It

Table 3 Summary of the uncertainty values for each of the load steps. The uncertainty values listed are for the maximum strain of each load step

v_{avg} (μm)	$u(d_k)$ (μstrain)	u_{CS} (μstrain)	u_{CAL} (μstrain)	$\varepsilon^{Y\,max} - \varepsilon^{Y\,min}$ (μstrain)	u_{rel} (%)
27.5	13	5	14.0	289	4.8
110	17	6	18.3	1103	1.7
218	27	8	28.7	2110	1.4

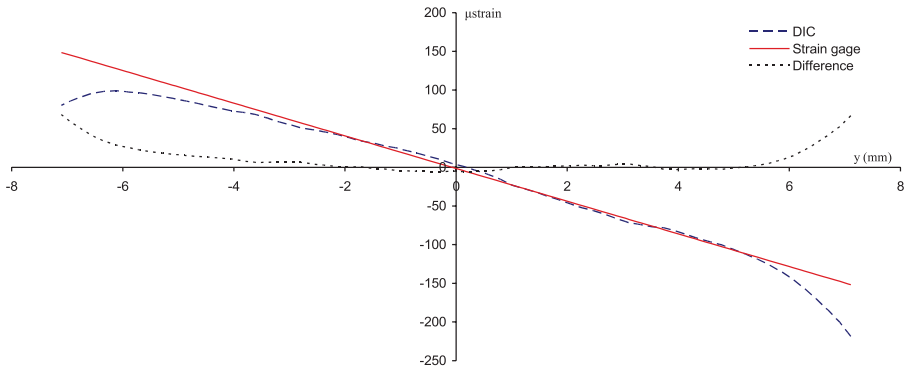

Figure 10 An initial measurement obtained for the 27.5 μm displacement load.

can be seen from this graph that there is a deviation in the measured versus predicted strain values as a function of the distance in the *y*-direction from the centerline of the specimen. This error could have arisen from a number of sources including image or spatial distortions; however, it was corrected first, by ensuring that the surface stayed flat when preparing it with the grit paper by using a sanding block. Initially, the surface was sanded by hand, which may have rounded the edges slightly, causing error in the measurements. And second, the camera was rotated by 90° which aligned the sensor's higher resolution dimension with the *y*-axis of the gage section and also allowed the camera to be moved closer to the specimen.

The applicability of this calibration is restricted to the spatial and strain scales for which it was performed, that is the instrument can only be considered to be calibrated for the analysis of strain in a field of view of comparable size and containing comparable strains as those shown in Figs. 4 and 6. If it is desired to use the instrument beyond these parameters then a new calibration would need to be performed, probably using a different reference material. The design of the reference material is parametric and hence can be scaled in size to provide different fields of view and strain levels. This calibration was performed using a speckle pattern consisting of a set of scratches rather than the more usual approach of a painted or printed speckle pattern. It is likely that the calibration is applicable only to similar scratch-based speckle patterns and that if a painted or printed pattern is to be used then a new calibration should be performed.

Conclusions

The results of calibrating a DIC system have been presented according to the procedure described by the SPOTS guideline. The system was shown to achieve an acceptable calibration as defined by the guideline and the minimum uncertainty for future measurements made with the optical setup was evaluated as 5% for maximum strains of the order of 120 μstrain and 1.4% for maximum strains of the order of 1000 μstrain. The calibration provides confidence for future strain measurements made with the system, and establishes traceability for the measurements to the international standard for length. The latter is important when analyses are associated with regulatory procedures. In addition, the procedure was performed using only the bare metal of the specimen, without the need to paint the surface with a speckle pattern. Some of the challenges of the procedure have been discussed.

References

1. ASME V&V 10-2006, *Guide for Verification and Validation in Computational Solid Mechanics*, *American Society of Mechanical Engineers*, New York (2006).
2. American Society for Testing and Materials, *C1377-97 Standard Test Method for Calibration of Surface/Stress Measuring Devices* (2003).
3. Standardised Project for Optical Techniques of Strain Measurement (SPOTS), ''Guidelines for the Calibration and Evaluation of Optical Systems for Strain Measurement,'' URL www.opticalstrain.org (2010).
4. Patterson, E.A., Hack, E., Brailly, P., et al. ''Calibration and Evaluation of Optical Systems for Full-Field Strain Measurement,'' *Optics and Lasers in Engineering* **45**:550–564 (2007).
5. International Organization for Standardization, *ISO10012-1, Quality Assurance Requirements for Measuring Equipment, Part 1: Metrological Confirmation System for Measuring Equipment* (1992).
6. Sutton, M.A., Orteu, J.J., and Schreier, H., *Image Correlation for Shape, Motion and Deformation Measurements: Basic Concepts, Theory and Applications*,Springer Verlag, New York, (2009).

7. Lopez-Crespo, P., Shterenlikht, A., Patterson, E.A., Yates, J.R., and Withers, P.J., ''The Stress Intensity of Mixed Mode Cracks Determined by Digital Image Correlation,'' *Journal of Strain Analysis for Engineering Design* **43**(8):769–780 (2008).
8. Lopez-Crespo, P., Burguete, R.L., Patterson, E.A., Shterenlikht, A., Withers, P.J., and Yates, J.R., ''Study of a Crack at a Fastener Hole by Digital Image Correlation,'' *Experimental Mechanics* **49**:551–559 (2009).
9. Grant, B.M.B., Stone, H.J., Withers, P.J., and Preuss, M., ''High-Temperature Strain Field Measurement Using Digital Image Correlation,'' *Journal of Strain Analysis for Engineering Design* **44**(4):263–271 (2009).
10. Bay, B.K., ''Texture Correlation: A Method for the Measurement of Detailed Strain Distributions Within Trabecular Bone,'' *Journal of Orthopaedic Research* **13**(2):258–267 (1995).
11. Quinta da Fonseca, J., Mummery, P.M., and Withers, P.J., ''Full-Field Strain Mapping by Optical Correlation of Micrographs Acquired During Deformation,'' *Journal of Microscopy* **218**(1):9–21 (2005).
12. Whelan, M.P., Albrecht, D., Hack, E., and Patterson, E.A.. ''Calibration of a Speckle Interferometry Full-Field Strain Measurement System,'' *Strain* **44**:180–190 (2008).
13. Herbst, C., and Splitthof, K., ''Basics of 3D Digital Image Correlation,'' *Technical Report T-Q-400-Basics-3DCORR-002a-EN*, Dantec Dynamics GmbH, Ulm, Germany.
14. Becker, T., Splitthof, K., Siebert, T., and Kletting, P., ''Error Estimations of 3D Digital Image Correlation Measurements,'' *Technical Report T-Q-400-Accuracy-3DCORR-003-EN*, Dantec Dynamics GmbH, Ulm, Germany (2006).